Nanoscale thermal conductivity spectroscopy by using gold nano-islands heat absorbers.

Takafumi Oyake[1], Masanori Sakata[1], and Junichiro Shiomi[1, 2a)]

[1]Department of Mechanical Engineering, The University of Tokyo, 7-3-1 Hongo, Bunkyo-ku, Tokyo 113-8656, Japan

[2]PRESTO, Japan Science and Technology Agency, 4-1-8 Honcho, Kawaguchi, Saitama 332-0012, Japan

ABSTRACT:

A measurement technique of quasi-ballistic thermal transport in tens of nanometers has been developed by using time-domain thermoreflectance of gold nano-islands. The suppressed apparent thermal conductivity of transparent substrates (fused quartz, crystal quartz, and sapphire) due to quasi-ballistic thermal transport is obtained through the transient temperature change of the gold nano-islands formed on the substrate surface, and the size effect of thermal conductivity in the range of tens of nanometers is quantified by varying the gold nano-island sizes. Furthermore, characteristic phonon mean free paths of the substrates were obtained by fitting the measured size effect with a solution of a Boltzmann transport equation. The results identify that the size-effect of amorphous fused quartz at room temperature becomes significant when the size is reduced below 60 nm.

[a)] Authors to whom correspondence should be addressed. E-mail: shiomi@photon.t.u-tokyo.ac.jp

Nondiffusive thermal transport occurs when characteristic lengths of systems are comparable to or smaller than phonon mean free paths (MFPs)[1–3]. Nondiffusive (or more specifically quasi-ballistic) thermal transport in nanostructures enhances the influence of interfaces and surfaces, and the resulting reduction in effective thermal conductivity is widely utilized for instance to improve the conversion efficiency of thermoelectric materials[4–6]. The quasi-ballistic thermal transport also plays a crucial role in thermal management of semiconductor devices, where heat flux from the hot spot is suppressed compared with the Fourier's law as the size of a hot spot approaches the phonon MFPs[7]. Therefore, knowledge in phonon MFPs is essential to engineer materials and systems for preferred thermal performance.

While the recent advances in numerical calculations[8,9] greatly progressed understanding of phonon MFPs in pure crystals, experimental measurements are indispensable to validate them, and, more importantly, to extend the knowledge to more complex structures such as amorphous. It has been possible to measure the size effect in thermal conductivity of thin films and nanowires, however, the size effect strongly depends on phonon scattering conditions at surfaces and interfaces[10], which need to be modeled in order to extract phonon MFPs. Recently, this has been overcome by *boundary-less* methods that measure suppression of apparent thermal conductivity of bulk material by localizing the measurement area/volume using optical techniques. The fundamental concept was first demonstrated by Koh *et al.*[11] in their time-domain thermoreflectance (TDTR) measurements of semiconductor alloys with a variation in pump-beam modulation frequencies (0.1 to 10 MHz), i.e. in thermal penetration depths. They showed that phonons with MFPs larger than the thermal penetration depth do not contribute to the apparent thermal

conductivity extracted from the measurements. More recently, Regner *et al.*[12] refined the method using frequency-domain thermoreflectance with higher modulation frequencies up to 200 MHz to scan broader range of phonon MFPs. In addition to thermal conductivity accumulation function of various crystalline materials, they found that, even in amorphous silicon, phonon-like propagating modes with MFP exceeding 100 nm can contribute to about 35% of the overall thermal conductivity.

There have also been methods with more explicit control over the measurement area/volume. Siemens *et al*.[13] used nanometer-sized metallic grating array as the heat absorbers. The soft X-ray probes the temporal signal of the diffracted beam due to transient heating of the metallic heat absorbers. This enabled them to observe thermal conductivity suppression due to phonons with MFPs as small as 65 nm, and thus to extract phonon MFPs of low thermal conductivity materials such as fused quartz and sapphire. Later, Minnich *et al.*[14] varied the heated area in TDTR by changing the laser-spot size, and showed that the measured size effect of silicon at cryogenic temperatures is consistent with that of first principles calculations. While the laser diameter is limited by the optical diffraction limits, Johnson *et al.*[15] developed the transient thermal grating method, where with interference of two pump laser beams effectively realizes a local heat source as small as 1 μm.

The above methods measure the suppression of apparent thermal conductivity due quasi-ballistic thermal transport, and the obtained size-dependence of thermal conductivity can be thought as an accumulation function of contribution to bulk thermal conductivity from phonons with various mean free paths[16]. In this sense, the measurements have been addressed as the *thermal*

conductivity spectroscopy. While most of the reported measurements so far have been performed on solids with fairly high thermal conductivity i.e. long phonon MFPs, the next nontrivial challenge is to develop a method for low thermal conductivity solids with short MFP phonons, which requires measurements at the scale of at least tens of nanometers. In this work, we develop a thermal conductivity spectroscopy method with bottom-up self-assembly approach, which can access the tens-of-nanometers scale. Being based on bottom-up self-assembly, the method in theory has potential to reach even nanoscale.

To localize and vary the measurement region at the scale of tens of nanometers, we form gold nano-island (GNIs)[17,18] on the transparent substrates and use them as heat absorber and reflector for the TDTR measurement. GNIs were formed by annealing a-few-nanometers-thick gold films deposited on the substrate surface. The geometrical and optical properties of GNIs have been investigated by theoretical calculations, cross-sectional transmission microscopy, and plasmonic absorption spectrum[17,18]. Unlike gold nanoparticles dispersed on a substrate[19], GNIs, being truncated spheres formed from a firmly deposited gold thin film, realize immobile area contact with the substrate. The size of the GNIs and contact diameter can be controlled in the range of tens of nanometers by changing the thickness of the gold thin film and the annealing temperature.

Firstly, 5-, 7-, and 9-nm-thick gold films were deposited on fused quartz, crystal quartz, and sapphire substrates, and then annealed in a furnace at 500 or 900 °C for 3 hours to form GNIs. After the formation of GNIs, the height and number density of GNIs were measured by the atomic force microscope (AFM). A typical AFM image of GNIs on sapphire substrate and distribution of their heights are shown in Fig. 1 (a) and (b), respectively. The average heights of GNIs on each substrate

were obtained from a 2 × 2 μm^2 AFM image. Now the key issue is how to identify the average contact diameter between GNIs and the substrate. In this work, this was done in two different ways. One is to measure the central angle of the truncated spheres using UV-Vis-NIR absorption spectra[17,18]. This utilizes the correlation between the central angle and the shift in the plasmonic absorption peak previously identified for GNIs on a fused quartz substrate. In cases of GNIs formed by annealing 7-nm-thick gold films on fused quartz substrates at 500 and 900 °C, the central angles of GNIs are estimated to be 92° and 115° from the absorption spectra shown in Fig 2 (a). Then together with the average heights, the contact diameters are obtained to be 37 and 27 nm, respectively.

The other way to obtain the contact diameter is to use the information of the average volume of a GNI. This can be estimated by dividing the total volume of the deposited gold film measured by a crystal oscillator with the number of GNIs measured by AFM. Combined with the average height, this allows us to uniquely identify the average contact diameter. We confirmed that the contact diameters obtained by the two different approaches agree well with each other for the case of fused quartz. Therefore, for the sake of simplicity, we have adopted the latter approach, which is more facile and versatile, on measuring the contact diameters of the rest of the samples. As shown in Fig. 2 (b) for the case of fused quartz, the contact diameters range from 25 nm and 80 nm, which are smaller than the previous work[13].

We use a TDTR method[1,2,20,21] to measure the transient thermal response of GNIs on the transparent substrates. TDTR is a pump-probe optical technique which is well established for measuring nanoscale thermal transport properties, such as size effect of thermal conductivity and

thermal boundary conductance (TBC). A Ti:Sapphire femtosecond laser emits pulses with a wavelength of 800 nm and duration of 140 fs at a repetition frequency of 80 MHz. The pulsed laser is then split into a pump beam (wavelength of 400 nm, 30 mW, 50 μm $1/e^2$ radius), which heats up the GNIs, and a probe beam (wavelength of 800 nm, 5 mW, 15 μm $1/e^2$ radius), which measures the transient thermal response at the surface of GNIs as a function of delay time between the pump and probe beam. The spot size of the pump beam is much larger than the GNIs, and hundreds of GNIs are simultaneously heated up by the beam. The pump beam is weak enough that the temperature rise at GNIs is less than 1 K. The pump beam is modulated at 11 MHz, and it heats only GNIs because substrates are transparent. The change of reflectivity R of GNI surface is measured by the photodiode and translated to temperature through thermoreflectance. The coefficient of thermoreflectance (dR/dT) of gold is relatively small (less than 10^{-4} K^{-1}), therefore the signal-to-noise ratio is enhanced by using a lock-in amplifier. The arrival time of the probe beam at the surface of the sample is adjusted using a mechanical delay stage to measure the reflected intensity as a function of delay time.

The target thermal properties were extracted by fitting the measured TDTR signal with a solution of a heat conduction model. The heat conduction model and fitting methodology have been fully established and described in the literature[20,21]. Here, the model requires inputs such as geometry, heat capacity, thermal conductivity of GNIs, and heat capacity of the substrate. We take the bulk heat capacity and thermal conductivity of gold for GNIs, and similarly the bulk heat capacity for the transparent substrates. Note that the fitting sensitivity to the thermal conductivity of GNIs is small compared to the other parameters because temperature of GNIs quickly reaches

thermal equilibrium, therefore accuracy of the GNI thermal conductivity is not important. The actual locations of GNIs are not ordered, however, for the sake of simplicity, it was modeled with an aligned GNI array [Fig. 3 (a)] with the pitch *p* giving the same number density as the actual GNIs. Furthermore, the partially spherical GNI was modeled by a cuboid with the width *d* corresponding to the contact diameter and height *h* determined to give the same average volume with that of the actual GNIs.

The fitting was performed for the amplitude signal from the lock-in amplifier. Typical signals and best-fit curves are shown in Fig. 3(b). Here, the data are normalized by the value at 100 ps. The signal from 100 ps to 2 ns was used for the fitting. The averaged TBC of GNIs/substrate interface and the suppressed thermal conductivity of the substrate are the fitting parameters, and determined by minimizing the least-squared error between the measured and modeled signals.

The obtained TBC values in the cases of fused quartz, crystal quartz, and sapphire substrates are 82 ±14 $MWm^{-2}K^{-1}$, 93 ± 17 $MWm^{-2}K^{-1}$ and 110 ± 26 $MWm^{-2}K^{-1}$, respectively. Each value of TBC was independent of the average size of GNIs, which assures that the same thermal contact is realized when changing the contact diameter. The measured thermal conductivities of fused quartz, crystal quartz, and sapphire are shown in Fig. 4 as a function of the contact diameter. Thermal conductivity here is normalized with the bulk value. Error bars indicate the standard deviation of measurement accounting for the distribution of contact diameter. The suppression of thermal conductivity is captured, which assures that the contact diameter is small enough in comparison with the phonon MFPs to probe the quasi-ballistic thermal transport.

To extract the characteristic phonon MFP from the measurement results, we use the solution of

Boltzmann transport equation (BTE). We adopted Chen's model[7] of the ballistic phonon transport from an embedded hotspot into an infinite substrate, whose geometry is essentially the same as the current case if we assume that a GNI generates a hemispherical hotspot at the substrate surface. Then the suppressed thermal conductivity (κ_{eff}) normalized by the bulk value (κ_{bulk}) can be expressed as $\kappa_{eff} / \kappa_{bulk} = \tau / (\tau + 4/3)$, where τ is the hot spot radius divided by the characteristic phonon MFP of the medium. Note that MFP of phonon in crystals should depend on the phonon mode, however, we have employed a single effective MFP to also account for amorphous materials, where it is not clear how relevant the picture of mode-dependent phonon propagation is[22,23].

The expression was fitted to our experimental data with the phonon MFP as a single fitting parameter. As shown in Fig. 4, the residual of the fitting is the smallest for case of sapphire. The obtained profile also agrees well with the values of Minnich measured by TDTR with dot arrays as small as 400 nm fabricated by electron beam lithography[24]. As a result, the phonon MFPs of fused silica, crystal quartz, and sapphire are identified to be 3.5 nm, 9.4 nm, and 84 nm, respectively. The phonon MFP of sapphire also agrees well with 120 nm reported by Siemens *et al.*[13], which confirms the credibility of the current measurement method. In addition, to make sure that the measurements capture the proper temperature dependence of phonon MFP, we have also measured sapphire substrates at 100 K, as shown in Fig. 4. The measurements confirm that the size effect of the thermal conductivity is much stronger at low temperature due to increase in the phonon MFP. The comparison with the BTE solution identifies the phonon MFP of 320 nm, which is in reasonable agreement with ~252 nm estimated from the room-temperature MFP (84 nm) assuming the inverse proportionality of phonon MFP to temperature. Note that the moderate overestimation is also

reasonable because the effective phonon frequency decreases with temperature, particularly for the high Debye-temperature material (1040 K), which causes some increase in the single effective MFP.

The phonon MFPs of fused quartz has been extracted by Siemens *et al.*[13] but the size effect was rather small compared to the measurement uncertainty because their length scale was limited to 65 nm. The thermal conductivity of Ref. 13 recalculated using their τ is shown in Fig. 4. Negligible thermal conductivity suppression for length scales larger than 60 nm was also reported by Regner *et al.*[12]. In contrast, the current results clearly identify the significant size effect bellow ~60 nm with capability to reduce the measurement length scale to 27 nm.

It is also interesting to point out that while our measured data agree with the solution of BTE within the error bars for the cases of sapphire and crystal quartz, the size effect of the measured thermal conductivity is much stronger than the BTE solution for the case of amorphous fused quartz even with the best fit. Note that this cannot be explained by the neglect of mode-dependence of MFP, since accounting for the mode-dependence would make the size effect of thermal conductivity weaker. The strength of the size effect appears even more anomalous if we in addition consider the thermal transport in the framework of Allen-Feldman theory[22], which predicts a significant contribution from non-propagating vibrational modes to thermal conductivity of amorphous fused quartz[25]. This encourages further theoretical studies of thermal conductivity suppression in amorphous structures with nanoscale MFPs.

In summary, quasi-ballistic thermal transport of transparent substrates have been investigated by the time domain thermoreflectance with gold nano-islands as heat absorbers. The average contact diameter of GNIs and substrates were controlled between 27 to 104 nm by the deposited gold

thickness and annealing temperature, and suppression of thermal conductivity was measured as a function of the contact diameter. Comparison of the analytical solution of Boltzmann transport equation with the suppressed thermal conductivity shows that phonon mean free paths of fused quartz, crystal quartz, and sapphire substrates are 3.5, 9.4, and 86 nm, respectively. Furthermore, the measurements identified that the thermal conductivity suppression of amorphous fused quartz becomes significant and even stronger than that predicted by phonon Boltzmann transport when the heated size becomes smaller than 60 nm.

ACKNOWLEDGMENTS

Part of this work was financially supported by Grants-in-Aid for Scientific Research (KAKENHI) 26709009 and 26630061, and Japan Science and Technology Agency PRESTO. T.O. was financially supported by Japan Society for the Promotion of Science (JSPS) Fellowship (26-9110) and through the Leading Graduates Schools Program, "Global Leader Program for Social Design and Management," by the Ministry of Education, Culture, Sports, Science and Technology.

REFEERENCES

[1] D.G. Cahill, W.K. Ford, K.E. Goodson, G.D. Mahan, A. Majumdar, H.J. Maris, R. Merlin, and S.R. Phillpot, J. Appl. Phys. **93**, 793 (2003).

[2] D.G. Cahill, P. V. Braun, G. Chen, D.R. Clarke, S. Fan, K.E. Goodson, P. Keblinski, W.P. King, G.D. Mahan, A. Majumdar, H.J. Maris, S.R. Phillpot, E. Pop, and L. Shi, Appl. Phys. Rev. **1**, 011305 (2014).

[3] E. Pop, Nano Res. **3**, 147 (2010).

[4] A.J. Minnich, M.S. Dresselhaus, Z.F. Ren, and G. Chen, Energy Environ. Sci. **2**, 466 (2009).

[5] A.I. Hochbaum, R. Chen, R.D. Delgado, W. Liang, E.C. Garnett, M. Najarian, A. Majumdar, and P. Yang, Nature **451**, 163 (2008).

[6] B. Poudel, Q. Hao, Y. Ma, Y. Lan, A. Minnich, B. Yu, X. Yan, D. Wang, A. Muto, D. Vashaee, X. Chen, J. Liu, M.S. Dresselhaus, G. Chen, and Z. Ren, Science **320**, 634 (2008).

[7] G. Chen, J. Heat Transfer **118**, 539 (1996).

[8] K. Esfarjani, G. Chen, and H.T. Stokes, Phys. Rev. B **84**, 085204 (2011).

[9] J. Shiomi, K. Esfarjani, and G. Chen, Phys. Rev. B **84**, 104302 (2011).

[10] P. Martin, Z. Aksamija, E. Pop, and U. Ravaioli, Phys. Rev. Lett. **102**, 125503 (2009).

[11] Y. Koh and D. Cahill, Phys. Rev. B **76**, 075207 (2007).

[12] K.T. Regner, D.P. Sellan, Z. Su, C.H. Amon, A.J.H. McGaughey, and J. a Malen, Nat. Commun. **4**, 1640 (2013).

[13] M.E. Siemens, Q. Li, R. Yang, K. a Nelson, E.H. Anderson, M.M. Murnane, and H.C. Kapteyn, Nat. Mater. **9**, 26 (2010).

[14] A.J. Minnich, J.A. Johnson, A.J. Schmidt, K. Esfarjani, M.S. Dresselhaus, K. a. Nelson, and G. Chen, Phys. Rev. Lett. **107**, 095901 (2011).

[15] J.A. Johnson, A.A. Maznev, J. Cuffe, J.K. Eliason, A.J. Minnich, T. Kehoe, C.M.S. Torres, G. Chen, and K.A. Nelson, Phys. Rev. Lett. **110**, 025901 (2013).

[16] A.J. Minnich, Phys. Rev. Lett. **109**, 205901 (2012).

[17] G. Gupta, D. Tanaka, Y. Ito, D. Shibata, M. Shimojo, K. Furuya, K. Mitsui, and K. Kajikawa, Nanotechnology **20**, 025703 (2009).

[18] G. Gupta, Y. Nakayama, K. Furuya, K. Mitsuishi, M. Shimojo, and K. Kajikawa, Jpn. J. Appl. Phys. **48**, 080207 (2009).

[19] M.-C. Daniel and D. Astruc, Chem. Rev. **104**, 293 (2004).

[20] D.G. Cahill, Rev. Sci. Instrum. **75**, 5119 (2004).

[21] A.J. Schmidt, X. Chen, and G. Chen, Rev. Sci. Instrum. **79**, 114902 (2008).

[22] P. Allen and J. Feldman, Phys. Rev. B **48**, 581 (1993).

[23] T. Hori, T. Shiga, and J. Shiomi, J. Appl. Phys. **113**, 203514 (2013).

[24] A.J. Minnich, Massachusetts Institute of Technology, PhD thesis, (2011).

[25] J.M. Larkin and A.J.H. McGaughey, Phys. Rev. B **89**, 144303 (2014).

FIGURES:

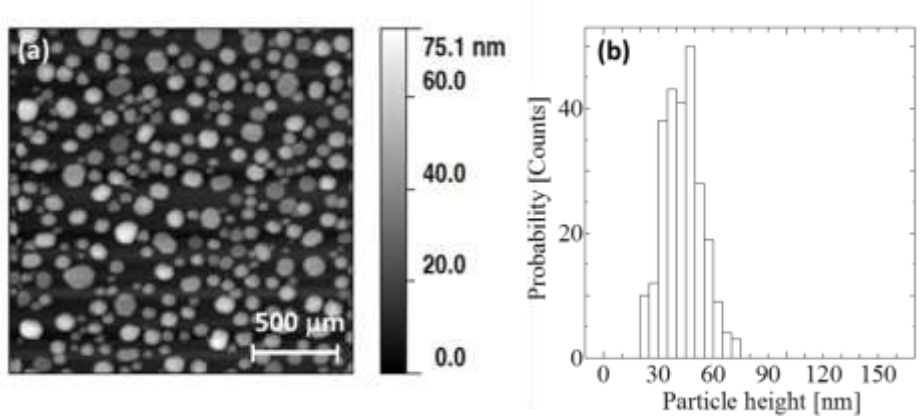

FIG. 1. Gold nano-islands synthesized by annealing 9 nm gold thin film at 900 °C on a sapphire substrate. (a) An atomic force microscope image, and (b) a histogram of particle height distribution. An average height and standard deviation are 43.2 nm and 10.6 nm, respectively.

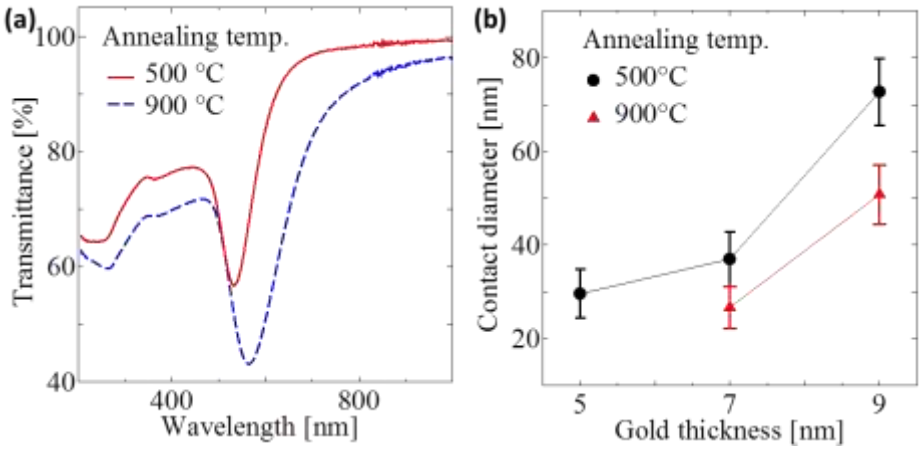

FIG. 2. (Color online) Contact diameters between GNIs and fused quartz substrates. (a) Absorption spectrum of GNIs on fused quartz substrate formed from the 7-nm-thick gold film. The central angle values are 92° and 115° estimated by the peak wavelength at 566 and 534 nm. (b) Contact diameter between GNIs and fused quartz substrate.

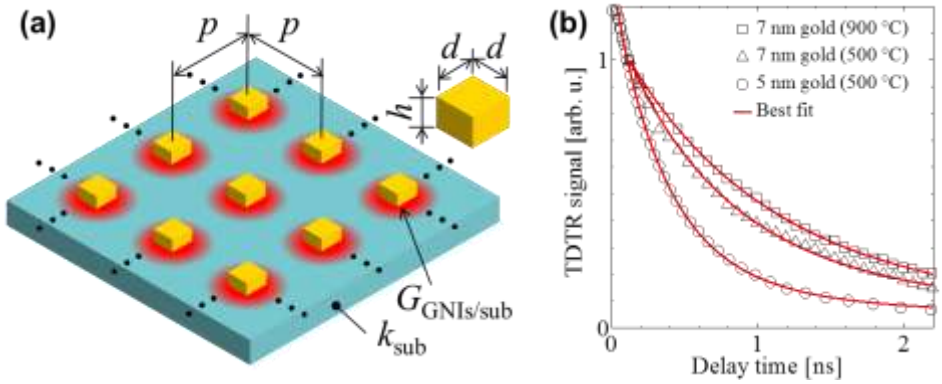

FIG. 3. (Color online) TDTR measurements of GNIs on transparent substrates. (a) A Schematic image of fitting model on TDTR measurement in this study. (b) Amplitude TDTR signals and best-fit profiles for GNIs on sapphire substrates formed by annealing 5- and 7-nm-thick gold films at 500 and 900 °C. Experimental signals are averaged over three different measurements.

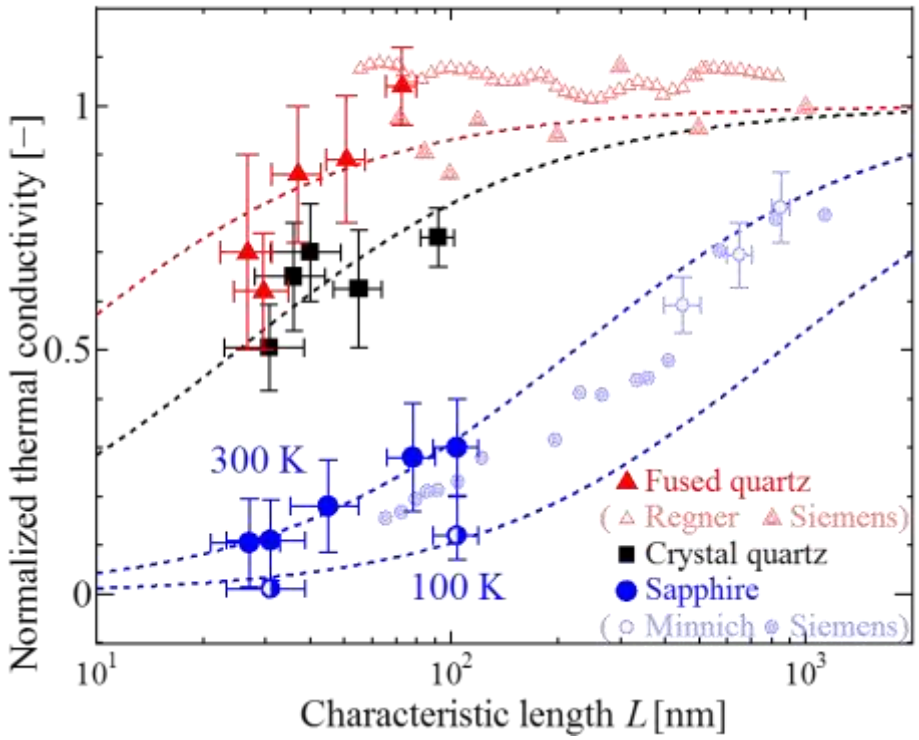

FIG. 4. (Color online) The normalized thermal conductivity of fused quartz (triangle), crystal quartz (square) and sapphire (circle) with respect to the contact diameter between GNIs and substrates. The dashed lines represent the best-fit solution of Boltzmann transport equation for fused quartz, crystal quartz and sapphire substrates. Open triangles and open circles are the values reported by Regner *et al*. and Minnich [24], respectively. Double triangle and double circles are the normalized

thermal conductivity reconstructed using τ values reported by Siemens *et al.* [13] through Chen's model [7].

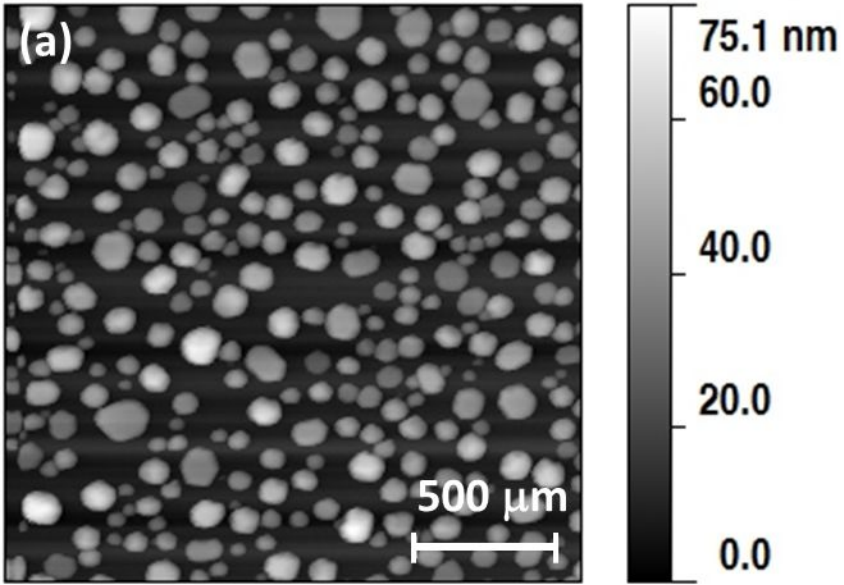
(a)
500 μm
75.1 nm
60.0
40.0
20.0
0.0

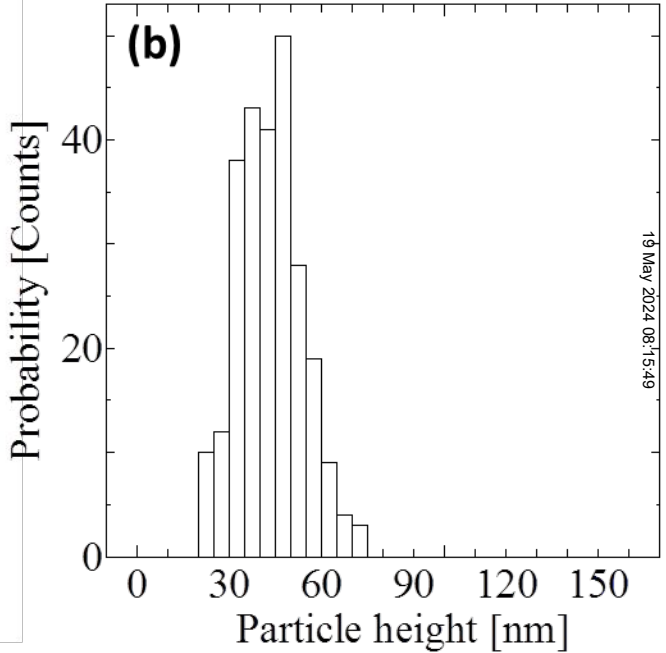
(b)
Probability [Counts]
0
20
40
0
30
60
90
120
150
Particle height [nm]
19 May 2024 08:15:49

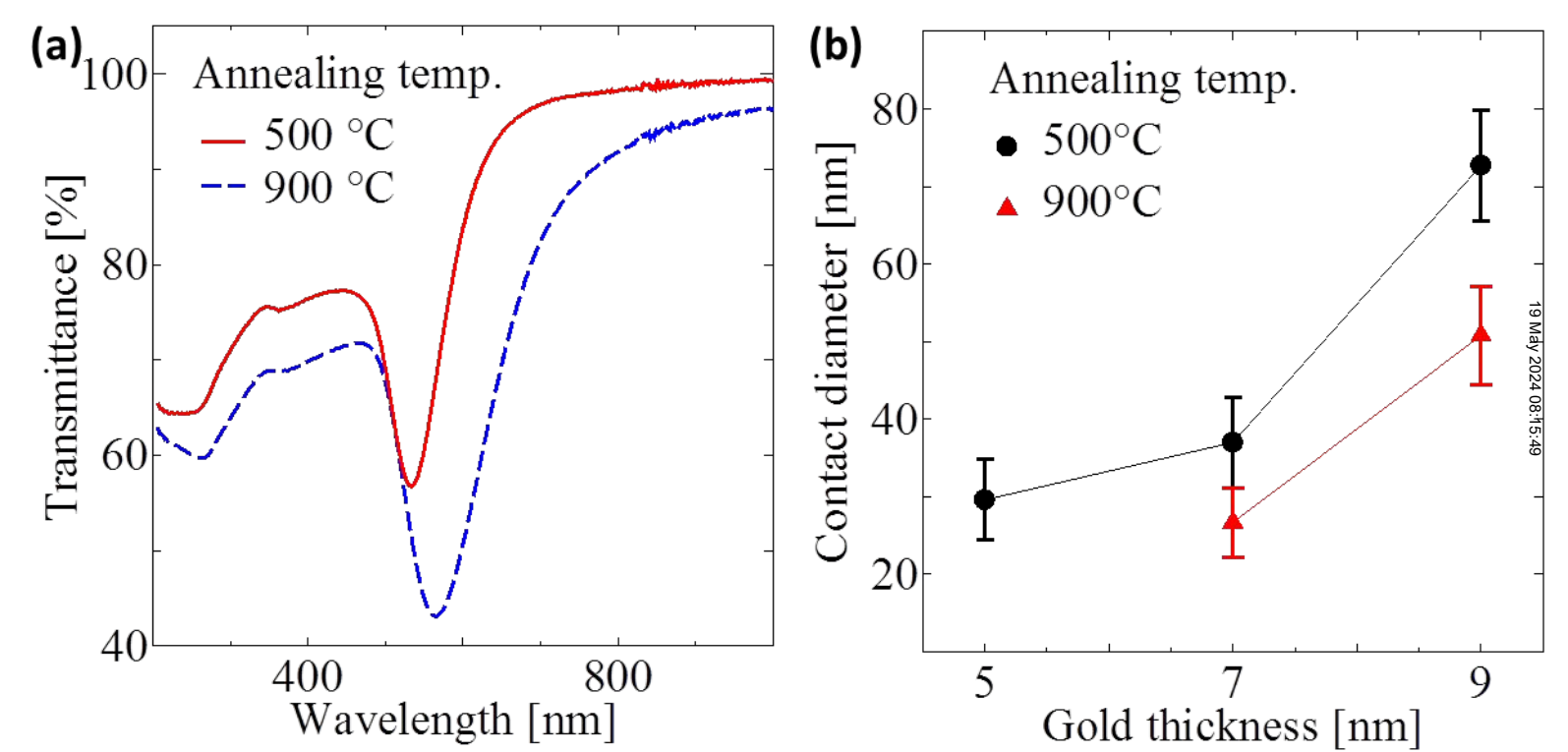
(a)
Annealing temp.
500 °C
900 °C
Transmittance [%]
100
80
60
40
400
800
Wavelength [nm]
(b)
Annealing temp.
500°C
900°C
Contact diameter [nm]
80
60
40
20
5
7
9
Gold thickness [nm]
19 May 2024 08:15:49

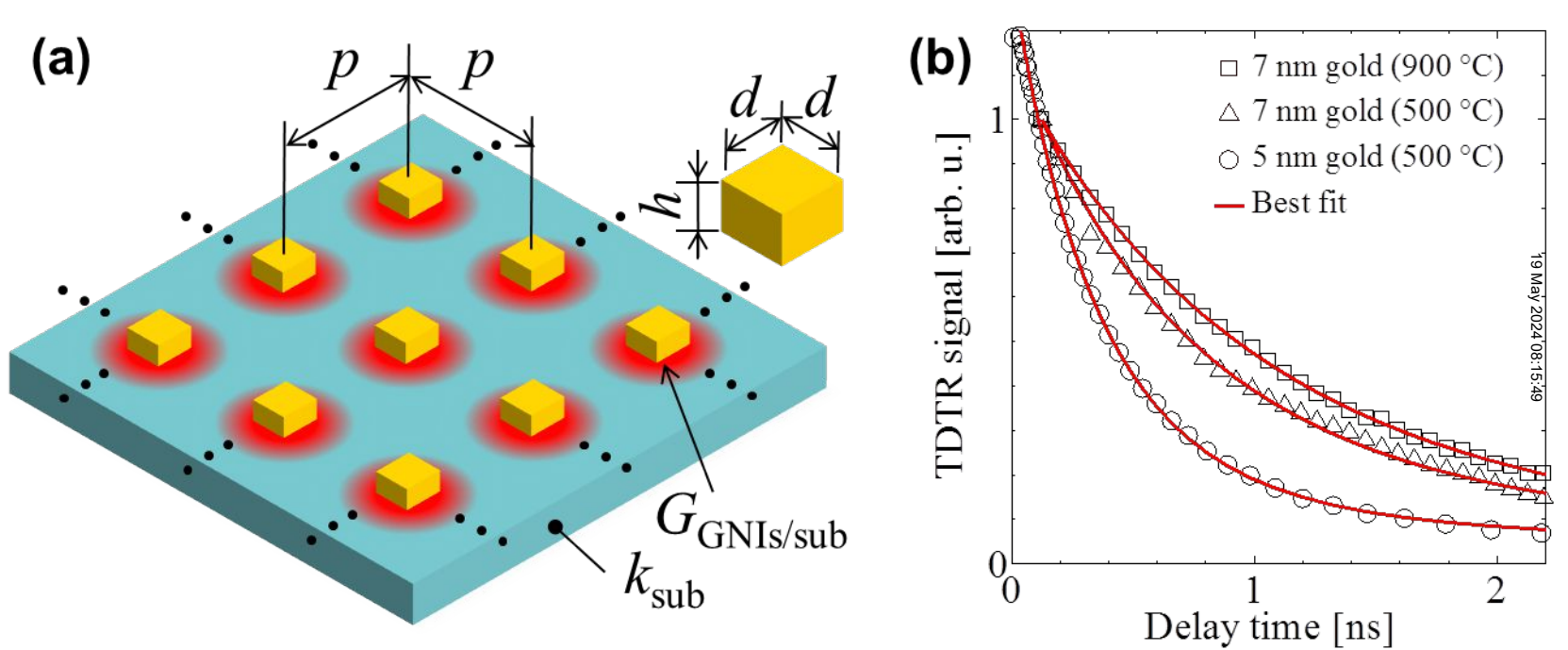
(a)
p
p
d
d
h
$G_{GNIs/sub}$
k_{sub}
(b)
7 nm gold (900 °C)
7 nm gold (500 °C)
5 nm gold (500 °C)
Best fit
TDTR signal [arb. u.]
Delay time [ns]
0
1
2
0
1
19 May 2024 08:15:49